

Monte Carlo Simulation and Static and Dynamic Critical Behavior of the Plane Rotator Model

Seiji MIYASHITA, Hidetoshi NISHIMORI, Akira KURODA^{*)} and Masuo SUZUKI

Department of Physics, University of Tokyo, Tokyo 113

(Received June 5, 1978)

The properties of phase transition and the lower-temperature phase of the plane rotator model are studied in the square lattice with Monte Carlo method. Physical results thus obtained for this model are quite similar to those of the two-dimensional quantum XY-model,¹⁾ that is, the susceptibility diverges and the specific heat does not diverge at the critical point. Furthermore the size-dependence of physical quantities and scaling relations among some temperature-dependent indices are also investigated.

§ 1. Introduction

In this decade, many investigations^{3)~17)} have been performed to clarify the physical properties of phase transition and in particular the low temperature phase of the two-dimensional XY-model as well as the plane rotator model, although these models have been rigorously proved to have no long-range order at any finite temperature.¹⁸⁾ Their Hamiltonians are given by

$$\mathcal{H}_{XY} = -J \sum_{\langle ij \rangle} (\sigma_i^x \sigma_j^x + \sigma_i^y \sigma_j^y) \quad (1.1a)$$

and

$$\mathcal{H}_{\text{p.l.r.}} = -J \sum_{\langle ij \rangle} \cos(\varphi_i - \varphi_j), \quad (1.1b)$$

respectively, where $\langle ij \rangle$ denotes the summation over all nearest neighbor bonds.

We have also studied the two-dimensional XY-model with Monte Carlo method.¹⁾ In this paper, we report physical properties of the plane rotator model in the square lattice obtained by the new Monte Carlo method proposed in a previous report.²⁾ In order to analyze critical behavior of the system, we investigate the size-dependence of physical quantities, in particular the susceptibility, specific heat and relaxation time. We conclude the appearance of the divergence of susceptibility and relaxation time, and non-divergence of specific heat. We also discuss the scaling relation between the temperature-dependent critical indices. The static properties are discussed in § 2. The dynamic properties and the scaling relation are discussed in § 3. The low temperature phase is considered with use of spin configurations in § 4. Finally conclusion and discussion are given in § 5.

^{*)} Permanent address: Faculty of Agriculture, Yamagata University, Tsuruoka, Yamagata.

§ 2. Static properties; susceptibility and specific heat

In this paper we discuss static properties of the plane rotator model. In order to find critical behavior clearly, we mainly discuss the following reduced susceptibility $\tilde{\chi}$ and specific heat \tilde{C} , namely,

$$N\tilde{\chi} \equiv N\chi k_B T = \langle M^2 \rangle - \langle M \rangle^2 = \langle (M - \langle M \rangle)^2 \rangle, \quad (2.1a)$$

$$N\tilde{C} \equiv NC(k_B T)^2 = \langle E^2 \rangle - \langle E \rangle^2 = \langle (E - \langle E \rangle)^2 \rangle, \quad (2.1b)$$

where T is the temperature and N is the total number of spins. These fluctuations of magnetization and energy are shown in Figs. 1 and 2, respectively. In Fig. 3, the temperature-dependence of energy is also shown. The energy shows extensivity very well.

The spontaneous magnetization $\langle M \rangle$ of our model should be zero. It takes, however, many Monte Carlo steps to realize this property at low temperatures, which is related to the fact that the time correlation function decays very slowly at lower temperatures than at a critical point T_{SK} . Under these situations we have found an interesting nature of $\langle M^2 \rangle$, that is, $\langle M^2 \rangle$ is rather stable against the number of Monte Carlo steps, as we can see in Table I. Thus, in order to obtain the susceptibility at low temperature, we propose the following physical assumption:

$$\langle M^2 \rangle_{400} \simeq \langle M^2 \rangle_{5000} \simeq \langle M^2 \rangle_{\infty}. \quad (2.2a)$$

However it should be noted that

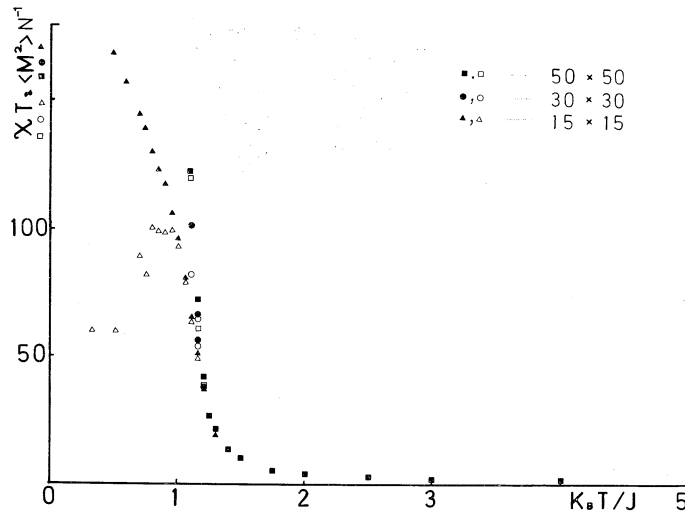


Fig. 1. Temperature- and size-dependence of the reduced susceptibility, $\tilde{\chi}$, and square of magnetization per spin, $\langle M^2 \rangle N^{-1}$ (see Eq. (2.1a)) at high temperature region. \square , \circ and \triangle denote the reduced susceptibility for $N=50 \times 50$, 30×30 and 15×15 , respectively. \blacksquare , \bullet and \blacktriangle denote the square of magnetization for $N=50 \times 50$, 30×30 and 15×15 , respectively.

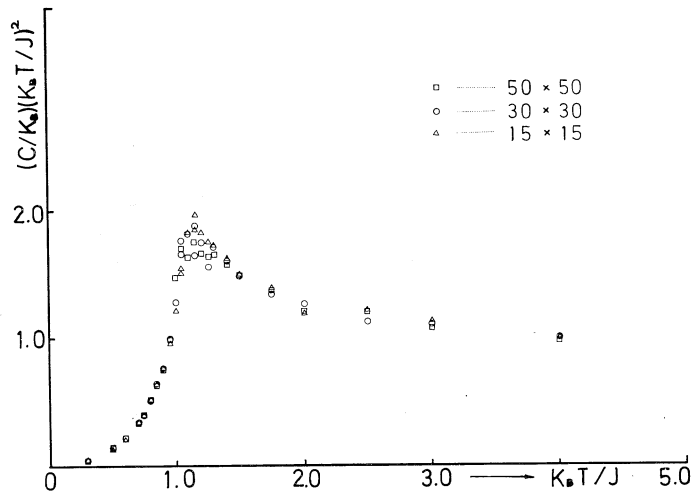


Fig. 2. Temperature- and size-dependence of the reduced specific heat, \tilde{C} (see Eq. (2.1b)). \square , \circ and \triangle denote the reduced specific heat for $N=50 \times 50$, 30×30 and 15×15 , respectively.

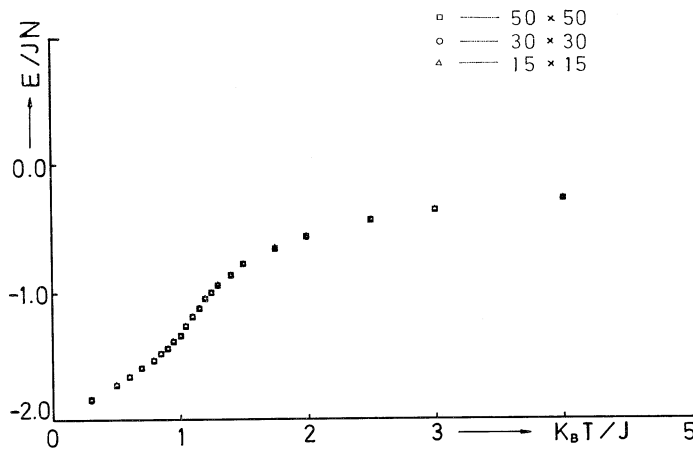


Fig. 3. Temperature- and size-dependence of the energy per spin, E/N , \square , \circ and \triangle denote the energy for $N=50 \times 50$, 30×30 and 15×15 , respectively.

Table I. Comparison of the values of $\langle M^2 \rangle N^{-1}$ averaged over 5000 Monte Carlo steps and 400 steps.

$k_B T/J$	N	15 \times 15		30 \times 30	
		$\langle M^2 \rangle_{5000} N^{-1}$	$\langle M^2 \rangle_{400} N^{-1}$	$\langle M^2 \rangle_{5000} N^{-1}$	$\langle M^2 \rangle_{400} N^{-1}$
1.2		40.616	44.559	46.097	44.365
1.1		64.899	65.888	103.295	127.1
1.0		95.700	98.188	267.391	—
0.9		118.046	110.127	398.432	361.88
0.75		144.581	139.487	497.843	472.72
0.50		170.450	170.275	634.831	—

$$\langle M \rangle_{400} \neq 0, \langle M \rangle_{5000} \simeq 0 \text{ and } \langle M \rangle_{\infty} = 0, \quad (2.2b)$$

namely $\langle M \rangle$ is not necessarily small at intermediate steps, and it goes to zero gradually. According to this physical proposition we may plot $\langle M^2 \rangle/N$ in Fig. 4 and regard $\langle M^2 \rangle/N$ rather than $(\langle M^2 \rangle - \langle M \rangle^2)/N$ as the reduced susceptibility at low temperatures, i.e., $k_B T < 1.0J$.

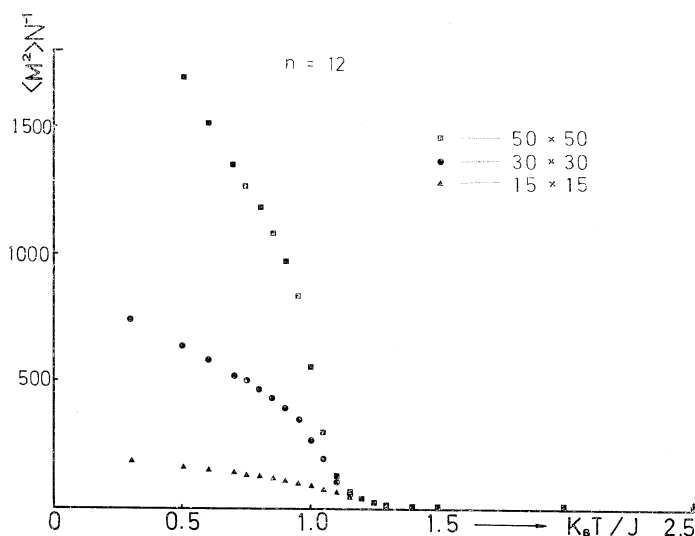


Fig. 4. Temperature- and size-dependence of the square of magnetization per spin, $\langle M^2 \rangle N^{-1}$ at low temperature region. \blacksquare , \bullet and \blacktriangle denote the square of magnetization for $N=50 \times 50$, 30×30 and 15×15 , respectively.

In Figs. 1 and 4, we can see the extensive property in the high temperature region, i.e., $k_B T > k_B T_{SK} \simeq 1.15J$, which indicates that this region corresponds to the paramagnetic phase. On the other hand, in the low temperature region, the size-dependence appears obviously, which indicates that this lower temperature region corresponds to another phase different from a paramagnetic one. In order to analyze the non-extensivity in this region, we assume the following size-dependence of the susceptibility per spin,

$$k_B T \chi = \frac{\langle M^2 \rangle}{N} = N^{a(T)}, \quad (2.3)$$

where N is the number of spins. This temperature-dependent exponent, $a(T)$, is plotted in Fig. 5. According to the previous work,^{(4), (7), (8)} the correlation $\langle S_0 S_r \rangle$ has the following form:

$$\langle S_0 S_r \rangle \propto r^{-\alpha(T)},$$

where $\alpha(T)$ depends on theories as follows:

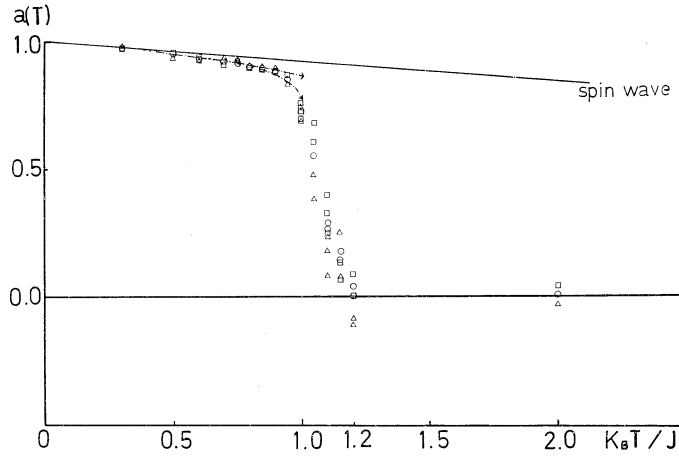


Fig. 5. Temperature-dependence of the index, $a(T)$, (see Eq. (2.3)) for the plane rotator model. \circ , \square and \triangle are corresponding to the values of $a(T)$ which are determined from the ratios,

$$\frac{\langle M^2 \rangle \text{ for system } N=50 \times 50}{\langle M^2 \rangle \text{ for system } N=15 \times 15}, \quad \frac{\langle M^2 \rangle; N=50 \times 50}{\langle M^2 \rangle; N=30 \times 30} \quad \text{and} \quad \frac{\langle M^2 \rangle; N=30 \times 30}{\langle M^2 \rangle; N=15 \times 15},$$

respectively.

$$\alpha(T) = \begin{cases} \frac{k_B T}{2\pi J}; \text{ spin wave theory}^4) \\ \frac{k_B T}{2\pi J} + (\text{vortex pair correction})^{\eta, 8); \text{ RG theory.} \end{cases} \quad (2.4)$$

Then, the susceptibility is represented as follows:

$$\begin{aligned} \chi k_B T &\sim \int_0^R \langle S_0 S_r \rangle dr = \int_0^R r^{1-\alpha(T)} dr \\ &\propto R^{2-\alpha(T)} \propto N^{1-\alpha(T)/2} \\ &\text{for } \alpha(T) < 2 \end{aligned} \quad (2.5)$$

in two dimensions. With (2.3) and (2.5), the two temperature-dependent indices relate to each other as

$$a(T) = 1 - \frac{\alpha(T)}{2} \quad (2.6)$$

in two dimensions. In Fig. 5, the exponent $a(T)$ of the spin wave theory is shown with a solid line.

Next we discuss the exponent η which is defined by

$$\langle S_0 S_r \rangle \sim \frac{1}{r^{d-2+\eta}} \quad (2.7)$$

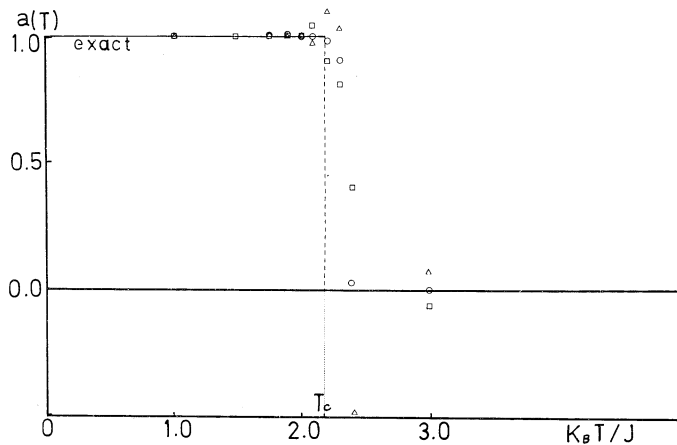


Fig. 6. Temperature-dependence of the index, $a(T)$, for the two-dimensional Ising model. \circ , \square and \triangle are the same symbols as in Fig. 5.

at the critical point. Consequently, η can be related to $\alpha(T)$ as

$$\eta = \alpha(T_{\text{SK}}) \quad (2.8)$$

in two dimensions ($d=2$). When we determine the value of η , we have to take account of an unavoidable error of the Monte Carlo method, that is, the ambiguity of determining sharp changes. This degree of uncertainty is demonstrated for the two-dimensional Ising model in Fig. 6. For the plane rotator model, we estimate the value of η from the extrapolation for the lower phase in Fig. 5 with dash-dotted lines. Thus we obtain

$$\eta = 0.25 \sim 0.5. \quad (2.9)$$

This result is consistent with the value of η obtained by other methods ($1/4^{(9,7)}$ and $1/\sqrt{8}$.¹⁰⁾ Here it should be noted that if we extrapolate from such a fairly low temperature region as “vortex-pair region” (see § 4), we obtain the value of η close to 0.25 and that if we extrapolate from higher temperature region, the value of η increases up to about 0.5.

Next we discuss the specific heat. As is seen in Fig. 2, the extensivity of it is satisfied in all temperature regions. Therefore, we conclude that the specific heat does not diverge at any temperature. The possibility of a weaker singularity is, however, not excluded. To confirm it definitely seems beyond the ability of Monte Carlo method. We can only say that the scattering of calculated values of specific heat becomes bigger and bigger, as the system size becomes larger and larger. This may be related to the instability of the variance of specific heat. In order to discuss the variance of specific heat, namely the fourth moment of energy, we need more precise data. It will be discussed in the near future.

§ 3. Dynamic properties and scaling relations

We study here the time correlation function, since it is such a typical quantity as characterizes time-dependent properties of a system. Below the critical point, the time correlation of the total magnetization is assumed to take the following form:

$$\langle M(0)M(t) \rangle \sim N^2 t^{-\Delta(T)}; \quad N = L^d, \quad (3.1)$$

where $\Delta(T)$ is given explicitly by

$$\Delta(T) = \Delta_{\text{SW}}(T) = k_B T / 4\pi J = \frac{1}{2} \alpha_{\text{SW}}(T), \quad (3.2)$$

in the spin wave region. The derivation of the above result (3.2) is given in the Appendix.

In order to discuss the scaling relation between the temperature-dependent indices $a(T)$ and $\Delta(T)$, we assume the following dynamic scaling form,

$$\begin{aligned} \langle M_q(0)M_q(t) \rangle N^{-1} &= \langle M_q^2(0) \rangle N^{-1} f(tq^{z(T)}) \\ &= \frac{1}{q^{2-\alpha(T)}} f(tq^{z(T)}) \\ &= \left(\frac{1}{q}\right)^d t^{-(d-2+\alpha(T))/z(T)} F(tq^{z(T)}), \end{aligned} \quad (3.3)$$

for small wave-number q , where

$$F(x) = x^{(d-2+\alpha(T))/z(T)} f(x).$$

In the limit of small q which is of the order of the inverse system size L^{-1} , the above correlation function may be reduced to the expression (3.1) for the correlation function of the uniform magnetization for finite size L . Thus, we arrive at the following scaling relation:

$$\Delta(T) = (d-2+\alpha(T))/z(T) \quad \text{or} \quad z(T)\Delta(T) + (2-\alpha(T)) = d. \quad (3.4)$$

If we use the relation $a(T) = 1 - \alpha(T)/d$, then we get

$$z(T)\Delta(T) + a(T)d = 2(d-1). \quad (3.5)$$

In particular, we have

$$z(T)\Delta(T) + 2a(T) = 2 \quad (3.6)$$

in two dimensions.

In fact, the above wave-number dependence of critical behavior, (3.3), can be interpreted as a finite size scaling relation through the relation

$$q \sim L^{-1} (L; \text{size}). \quad (3.7)$$

This has been discussed phenomenologically by Fisher¹⁹⁾ and also has been confirmed by Suzuki²⁰⁾ on the basis of renormalization group technique. Therefore, from the relaxation time for $M_q(t)$

$$\tau_q = \int_0^\infty \langle M_q(0) M_q(t) \rangle dt / \langle M_q^2(0) \rangle \simeq q^{-z(T)}, \quad (3.8)$$

we obtain the relaxation time of a finite system with size L of the form

$$\tau_L \sim (L^{-1})^{-z(T)} \sim L^{z(T)} \sim N^{z(T)/2}, \quad (3.9)$$

below the critical point in two dimensions. We can also obtain the field-dependence of the relaxation time using the scaling relation given by Berezinskii⁴⁾

$$\frac{1}{T} \Delta F(L, h) = L^d f\left(\frac{h}{T} L^{2-\alpha(T)/2}\right), \quad (3.10)$$

where ΔF is a singular part of the free energy. Applying the homogeneity relation between h and L , (3.10), we obtain the field-dependence of the relaxation time as follows:

$$\begin{aligned} \tau_h &\sim L^{z(T)} g\left(\frac{h}{T} L^{2-\alpha(T)/2}\right) \\ &\sim \left(\frac{h}{T}\right)^{-(z(T))/(2-\alpha(T)/2)} G\left(\frac{h}{T} L^{2-\alpha(T)/2}\right) \sim h^{-\omega(T)}, \end{aligned} \quad (3.11)$$

where

$$\omega(T) = \frac{z(T)}{2-\alpha(T)/2}$$

and

$$G(x) = x^{(z(T))/(2-\alpha(T)/2)} g(x). \quad (3.12)$$

It is very useful for numerical calculations that the whole range of temperature below T_{SK} is a critical line in two dimensions, as has been used in the above discussion.

Owing to the above relation, we investigate the size-dependence of the relaxation time, that is, we evaluate the exponent $z(T)$ defined in (3.9), instead of $\Delta(T)$ which is rather difficult to calculate with Monte Carlo method. The estimation of relaxation time, τ_L , is, however, very rough in our paper, so that we only discuss here the qualitative feature of it. We define numerically the relaxation time as the period of Monte Carlo steps in which the magnetization in a certain direction has the same sign, see Table II. From Table II, we find the following nature, that is, the relaxation time has size-dependence, and if we determine $z(T)$ as follows:

Table II. Comparison of the relaxation time τ of systems $N=50 \times 50$, 30×30 and 15×15 .

$k_B T/J$	N	15×15	30×30	50×50
1.20		less than 50	less than 50	100~ 50
1.15		70~ 50	100~ 50	150~ 50
1.10		200~ 50	250~100	350~100
1.05		300~100	350~100	550~100
1.00		500~200	900~300	1000~500
0.95		700~100	1200~500	more than 2000
0.90		1000~500	more than 2000	more than 2000

$$\left(\frac{N'}{N}\right)^{z(T)/2} = \frac{\tau_{N'}}{\tau_N}, \quad (3.13)$$

then we find numerically that $z(T)$ is much smaller than the value two which is predicted by the spin wave theory. If the exponent $z(T)$ does not depend on temperature, then the exponents $\Delta(T)$ and $\alpha(T)$ should have the same temperature-dependence through

$$\Delta(T) = \frac{1}{z} \alpha(T) = \frac{1}{2} \alpha(T); \quad z = z(0) = 2, \quad (3.14)$$

from (3.6), and consequently both static and dynamic critical exponents can be renormalized simultaneously with respect to temperature as

$$\Delta(T) = \Delta_{\text{SW}}^{(\text{eff})}(T) = \frac{1}{2} \alpha(T) = 1 - a(T) = -\frac{1}{4\pi J} k_B T_{\text{eff}}(T) \quad (3.15)$$

with use of an effective temperature $T_{\text{eff}}(T)$. However, as has been found from the analysis of (3.13), $z(T)$ depends on temperature and it is different from the value two obtained by the simple spin wave theory. Therefore we have to discuss the deviation of $\Delta(T)$ from the effective spin wave value $\Delta_{\text{SW}}^{(\text{eff})}(T)$ as

$$\Delta(T) - \Delta_{\text{SW}}^{(\text{eff})} = \alpha(T) \left(\frac{1}{z(T)} - \frac{1}{2} \right). \quad (3.16)$$

We find that $\Delta(T) > \Delta_{\text{SW}}^{(\text{eff})}$ since $z(T) < 2$ from our analysis, and that the difference between $\Delta(T)$ and $\Delta_{\text{SW}}^{(\text{eff})}$ increases as $z(T)$ becomes small.

Finally it should be noted that our analysis of the dynamical critical exponent $z(T)$ through (3.13) is based on global properties of dynamics of the system, while Ma²¹⁾ has used “local measurement” of time-dependent configurations in Monte Carlo simulations on the basis of renormalization group approach.

§ 4. Low temperature phase and spin configurations

In this section, we consider the low temperature phase and its spin configura-

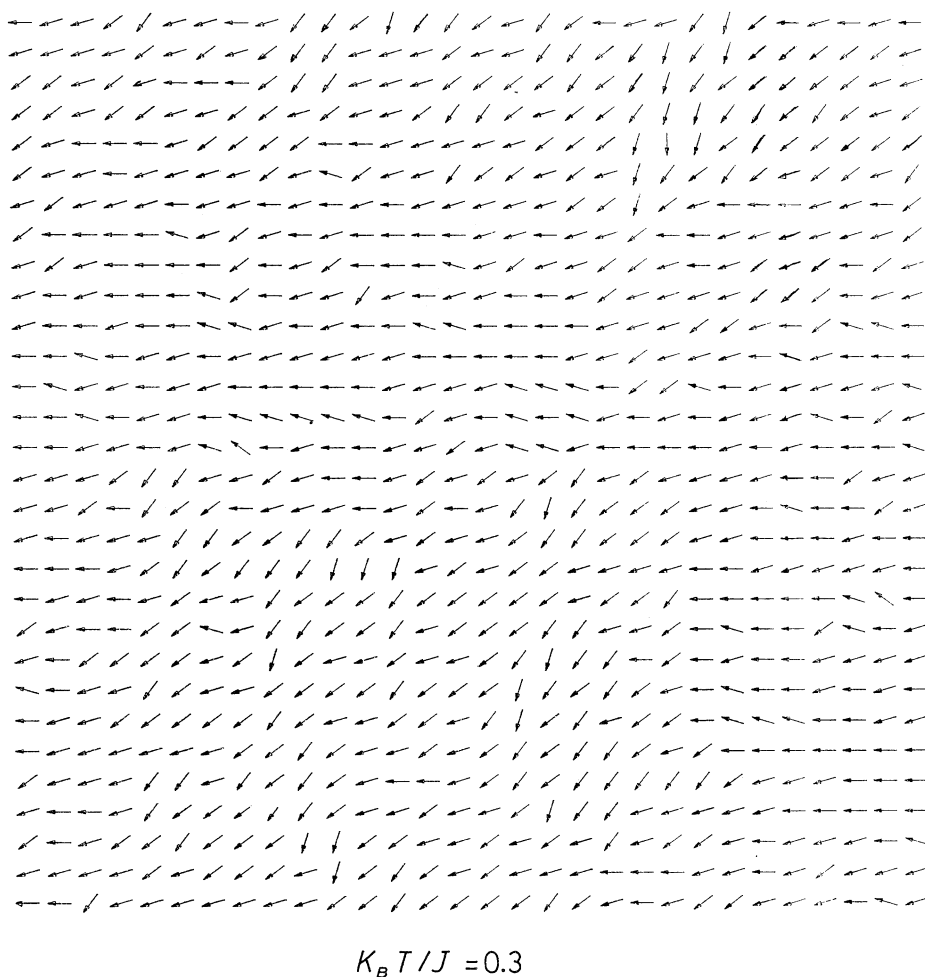


Fig. 7. Typical equilibrium spin configuration in the spin wave region, $k_B T = 0.3 J$ and Monte Carlo steps=2000.

tions. To investigate the low temperature phase, the harmonic approximation is used usually at very low temperatures. In this paper we call this region “spin wave region”, and the vortex pair correction is taken into account at a little higher temperature, whose region we call “vortex-pair region”. It may be interesting to show typical spin configurations corresponding to the above two regions. At very low temperatures, vortex-pairs exist, but the number of them is very small, as shown in Fig. 7. According to the terminology of Ref. 8), the vortex quantum number is 0. Next at a little higher temperature, the number of vortex-pairs increases. A typical configuration is shown in Fig. 8. In this region the vortex quantum numbers ± 1 are dominant. In Fig. 8, so-called vortex-pairs are indicated explicitly by broken lines. Our present Monte Carlo simulation has made

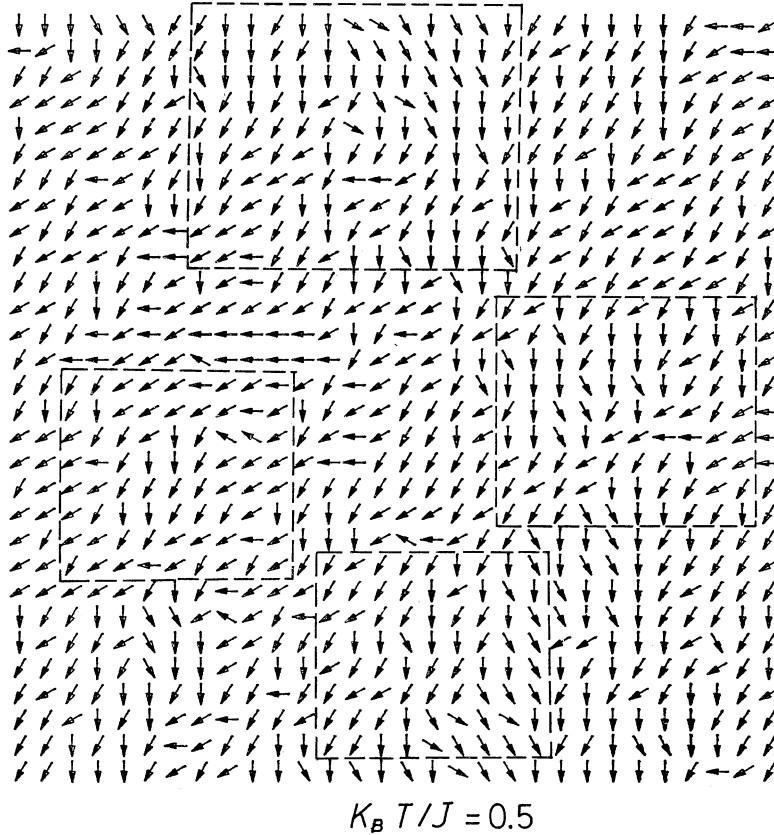


Fig. 8. Typical equilibrium spin configuration in the vortex-pair region, $k_B T = 0.5J$ and Monte Carlo steps=2000. The vortex-pairs are enclosed by broken lines.

it clear that the isolated vortex (see Fig. 9) does not appear at the equilibrium state, but only at a transient state. It is easy to imagine that the vortex with a positive quantum number, say $+1$ in Fig. 9, \bigcirc and with a negative quantum number, say -1 in Fig. 9, \bullet , combine to make vortex-pairs as in Fig. 4.

Next a typical spin configuration near the critical temperature is shown in Fig. 10. It seems difficult to say that it is enough to use the vortex-pair approximation at this region. Thus we believe that it is necessary to take higher vortex quantum numbers into account. It is natural to find that $k_B T_{SK} < 1.2J$ in our simulation while $k_B T_{SK} = (\pi/2)J = 1.57J$ in Refs. 7), 8), because higher excitations may cause the decrease of the critical temperature. Our result is consistent with upper bound of T_{SK} given by Myerson,¹⁵⁾ $k_B T_{SK} < 1.3J$. In other words, the screening effect of vortices seems to be essential near the critical temperature.

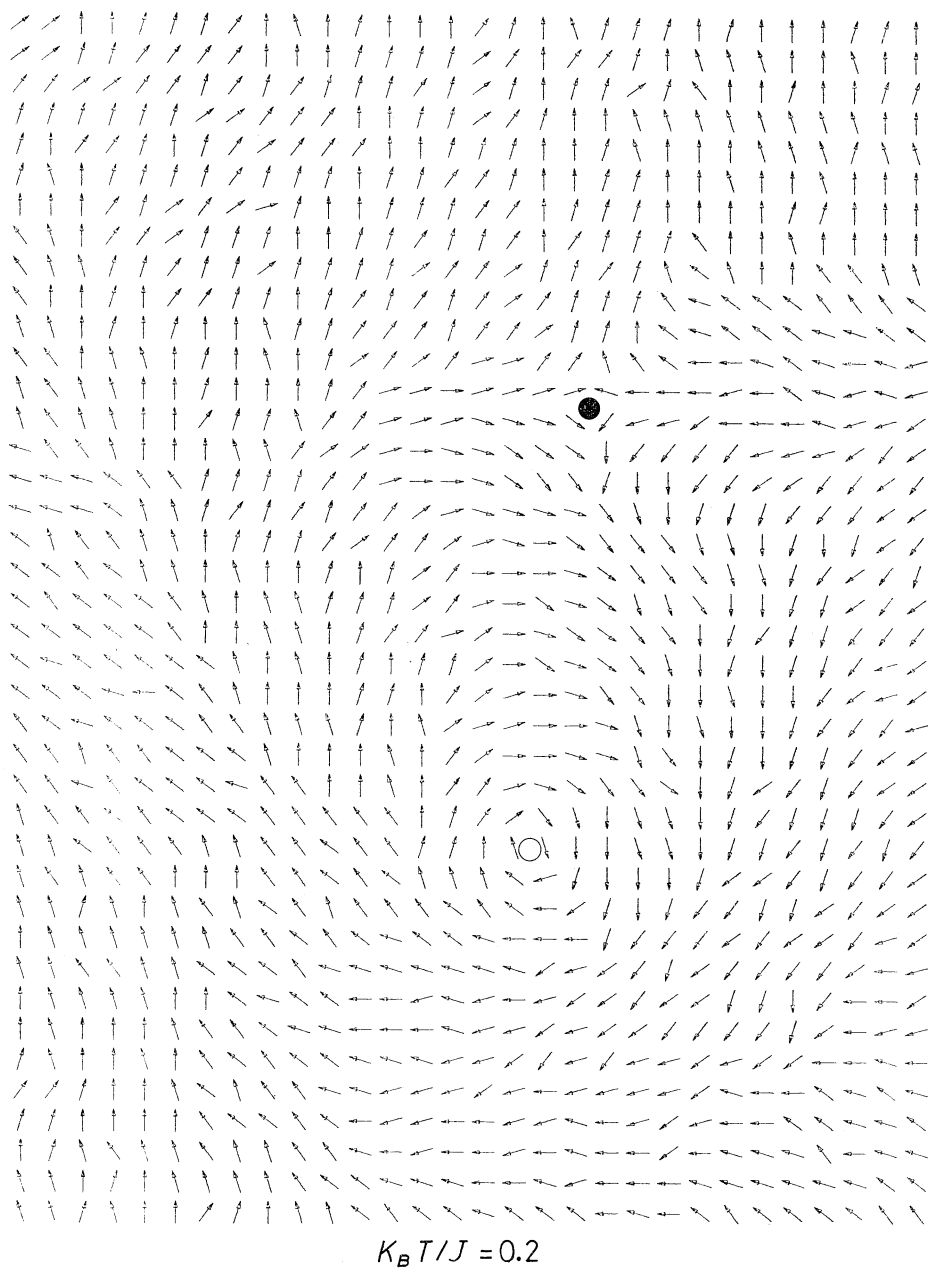


Fig.9. Typical spin configuration of isolated vortices. \circ and \bullet denote the centers of the isolated vortex with vortex quantum number $+1$ and -1 , respectively. $k_B T = 0.2J$ and Monte Carlo steps=30.

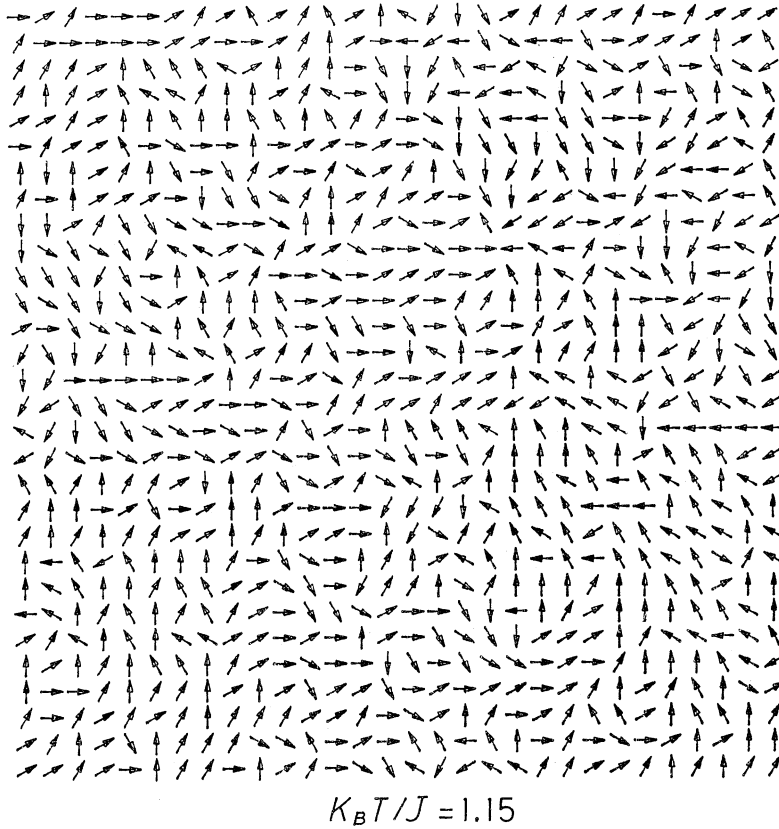


Fig.10. Typical equilibrium spin configuration near the critical point, $k_B T = 1.15J$ and Monte Carlo steps=2000.

§ 5. Conclusion and discussion

In this paper we have presented the temperature-dependence of energy, susceptibility or the average of square of magnetization $\langle M^2 \rangle$ and specific heat, and their size-dependence with Monte Carlo simulation. The susceptibility diverges at $k_B T_{SK} = 1.1J \sim 1.2J$ and we have found the interesting size-dependence. On the other hand, specific heat does not diverge. Dynamic properties, in particular the time correlation function and the size-dependence of relaxation time have been discussed.

Typical spin configurations at low temperatures have been shown and the vortex screening effect around the critical temperature has been discussed.

In this Monte Carlo simulation, we have used a new type of method,²⁾ that is, we introduced the discrete planar model whose discreteness is twelve, i.e., $n = 12$, $\theta_j = 2\pi k_j / n$, $k_j = 0, 1, 2, \dots, n-1$. The effect of the discreteness should appear only at very low temperatures and physical properties at temperatures of order J/k_B should not be affected by this discreteness. It seems quite reasonable to ac-

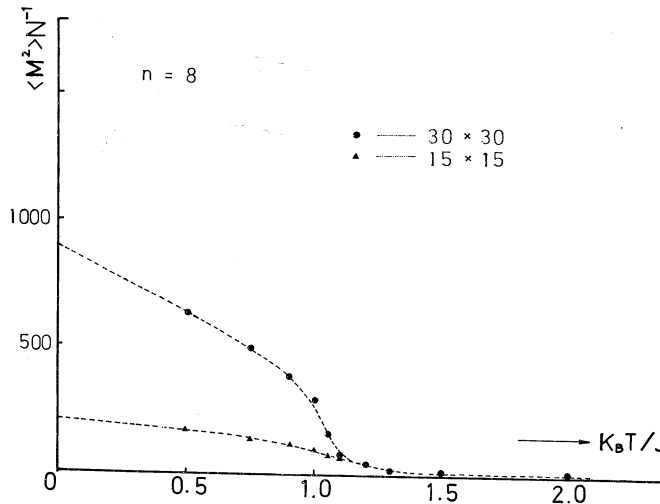


Fig. 11. Temperature- and size-dependence of the square magnetization per spin, $\langle M^2 \rangle N^{-1}$ for n (discreteness)=8. \bullet and \blacktriangle denote those for $N=30 \times 30$ and 15×15 , respectively. The broken line denotes the most probable value of the square magnetization for $n=12$, Fig. 4.

cept that $n=12$ is large enough to investigate physical properties of the continuous plane rotator model. A similar discreteness was discussed as an effect of symmetry breaking field in Ref. 8). In order to check this proposition, we have also simulated the model whose discreteness is eight, $n=8$. The results obtained for $n=8$ are given in Fig. 11 for the square of magnetization $\langle M^2 \rangle$, which agree with those for $n=12$. Other physical properties such as energy and specific heat, also agree with those for $n=12$ very well. Thus we conclude that physical properties of the discrete models do not depend on the discreteness n even for $n=8$ and 12 except at very low temperatures. Thus, it is believed that $n=8$ and $n=12$ discrete models should have the same physical properties as the continuous model near the critical point.

Acknowledgements

We would like to thank Professor R. Kubo and Professor D. D. Betts for their kind encouragement and useful discussions, and also thank Dr. F. Tanaka for his useful comments. We also thank Dr. Y. Kanada for his kind help concerning a high speed computer. This study is partially financed by Japanese scientific Research Fund of the Ministry of Education and Institute of Plasma Physics, Nagoya University (FACOM M190) and also by the National Research Council of Canada.

Appendix

Here we investigate the form of the time correlation function at low tempera-

tures. The following calculation in this appendix is, however, essentially given by Prudnikov and Teitelbaum²²⁾ for a system in which the total magnetization is conserved. Our Hamiltonian (1.1) can be rewritten at low temperatures as

$$\mathcal{H} \simeq \frac{J}{2} \int (\nabla \varphi)^2 d\mathbf{r}. \quad (\text{A} \cdot 1)$$

The stochastic Langevin equation has the following form with Hamiltonian (A.1):

$$\begin{aligned} \frac{\partial \varphi}{\partial t} &= -\gamma \frac{\delta \mathcal{H}}{\delta \varphi} + \eta \\ &= \gamma J \nabla^2 \varphi + \eta, \end{aligned} \quad (\text{A} \cdot 2)$$

where η is the Gaussian and white random force,

$$\langle \eta(\mathbf{r}, t) \eta(\mathbf{r}', t') \rangle = 2\gamma k_B T \delta(\mathbf{r} - \mathbf{r}') \delta(t - t'). \quad (\text{A} \cdot 3)$$

We rewrite (A.2) and (A.3) with $\varphi(\mathbf{k}, \omega)$ and $\eta(\mathbf{k}, \omega)$,

$$\begin{aligned} \varphi(\mathbf{k}, \omega) &= \int \varphi(\mathbf{r}, t) e^{i\mathbf{k}\mathbf{r} - i\omega t} d\mathbf{r} dt, \\ \eta(\mathbf{k}, \omega) &= \int \eta(\mathbf{r}, t) e^{i\mathbf{k}\mathbf{r} - i\omega t} d\mathbf{r} dt. \end{aligned} \quad (\text{A} \cdot 4)$$

(A.2) is rewritten as

$$(-i\omega + \gamma J k^2) \varphi(\mathbf{k}, \omega) = \eta(\mathbf{k}, \omega), \quad (\text{A} \cdot 5)$$

and (A.3) is rewritten as

$$\langle \eta(\mathbf{k}, \omega) \eta(\mathbf{k}', \omega') \rangle = (2\pi)^{d+1} 2\gamma k_B T \delta(\mathbf{k} + \mathbf{k}') \delta(\omega + \omega'). \quad (\text{A} \cdot 6)$$

From (A.5) and (A.6), we obtain

$$\begin{aligned} \langle \varphi(\mathbf{k}, \omega) \varphi(\mathbf{k}', \omega') \rangle &= \frac{2\gamma k_B T \delta(\mathbf{k} + \mathbf{k}') \delta(\omega + \omega') (2\pi)^{d+1}}{(-i\omega + \gamma J k^2) (-i\omega' + \gamma J k'^2)} \\ &= \frac{2\gamma k_B T \delta(\mathbf{k} + \mathbf{k}') \delta(\omega + \omega') (2\pi)^{d+1}}{|i\omega - \gamma J k^2|^2}. \end{aligned} \quad (\text{A} \cdot 7)$$

Thus, we get the correlation function of φ as follows:

$$\begin{aligned} \langle \varphi(\mathbf{r}, t) \varphi(0, 0) \rangle &= \frac{1}{(2\pi)^{2d+2}} \iint \langle \varphi(\mathbf{k}, \omega) \varphi(\mathbf{k}', \omega') \rangle e^{i\mathbf{k}\mathbf{r} - i\omega t} d\mathbf{k} d\omega d\mathbf{k}' d\omega' \\ &= \frac{1}{(2\pi)^{d+1}} \int \frac{2\gamma k_B T}{|i\omega - \gamma J k^2|^2} e^{i\mathbf{k}\mathbf{r} - i\omega t} d\mathbf{k} d\omega. \end{aligned} \quad (\text{A} \cdot 8)$$

As the random force η is Gaussian, $\varphi(\mathbf{r}, t)$ is also Gaussian. Therefore we can

derive the correlation function of spins as follows:

$$\begin{aligned}\langle \cos(\varphi(\mathbf{r}, t) - \varphi(0, 0)) \rangle &= \langle e^{i\{\varphi(\mathbf{r}, t) - \varphi(0, 0)\}} \rangle \\ &= e^{-(1/2)\langle (\varphi(\mathbf{r}, t) - \varphi(0, 0))^2 \rangle}.\end{aligned}\quad (\text{A}\cdot 9)$$

With (A·8), we obtain

$$\begin{aligned}\frac{1}{2}\langle (\varphi(\mathbf{r}, t) - \varphi(0, 0))^2 \rangle &= \frac{1}{2} \{ \langle \varphi^2(\mathbf{r}, t) \rangle + \langle \varphi^2(0, 0) \rangle \\ &\quad - 2\langle \varphi(\mathbf{r}, t) \varphi(0, 0) \rangle \} \\ &= \frac{1}{(2\pi)^3} \int \frac{2\gamma k_B T}{|i\omega - \gamma J k^2|^2} (1 - e^{-i\omega t + i\mathbf{k}\mathbf{r}}) d\mathbf{k} d\omega \\ &= \frac{1}{(2\pi)^2} \int \frac{k_B T}{J k^2} (1 - e^{-\gamma J k^2 t + i\mathbf{k}\mathbf{r}}) d\mathbf{k}\end{aligned}\quad (\text{A}\cdot 10)$$

in two dimensions. Let us consider the case, $\mathbf{r}=0$. (A·10) has the following form:

$$\frac{1}{2}\langle (\varphi(0, t) - \varphi(0, 0))^2 \rangle \simeq \frac{1}{2\pi K} \log(\pi\sqrt{t}); \quad K = \frac{J}{k_B T} \quad (\text{A}\cdot 11)$$

for large t . With (A·9) we obtain the time correlation function of the form

$$\langle \cos(\varphi(0, t) - \varphi(0, 0)) \rangle \simeq \exp\left(-\frac{1}{2\pi K} \log(\pi\sqrt{t})\right) \simeq C \cdot t^{-k_B T/4\pi J}. \quad (\text{A}\cdot 12)$$

Next we also consider the correlation function in equilibrium

$$\frac{1}{2}\langle (\varphi(\mathbf{r}, 0) - \varphi(0, 0))^2 \rangle \simeq \frac{1}{2\pi K} \log(r\pi) \quad \text{for large } r.$$

Then we obtain the same result as the spin wave theory,⁴⁾

$$\langle \cos(\varphi(\mathbf{r}, 0) - \varphi(0, 0)) \rangle \simeq r^{-(k_B T/2\pi J)}. \quad (\text{A}\cdot 13)$$

Finally let us consider the scaling relation and the index $z(T)$. With (A·12) and (A·13), the indices $\Delta(T)$ and $a(T)$ are given by

$$\Delta(T) = \frac{k_B T}{4\pi J} \quad \text{and} \quad a(T) = 1 - \frac{k_B T}{4\pi J}. \quad (\text{A}\cdot 14)$$

Consequently we obtain the relation

$$\Delta(T) + a(T) = 1 \quad (\text{A}\cdot 15)$$

in our spin wave approximation. Using the scaling relation (3·6), we conclude that the index $z(T)$ is two in this region.

References

- 1) M. Suzuki, S. Miyashita and A. Kuroda, Prog. Theor. Phys. **58** (1977), 1377.
- 2) M. Suzuki, S. Miyashita and A. Kuroda, Prog. Theor. Phys. **58** (1977), 701.
- 3) See D. D. Betts, in *Phase Transition and Critical Phenomena*, Vol. 3, edited by C. Domb and M. S. Green. (Academic Press, N. Y.).
- 4) V. L. Berezinskii, Soviet Phys.-JETP **32** (1971), 493.
- 5) J. Zittartz, Z. Physik **B23** (1976), 55, 63.
- 6) J. M. Kosterlitz and D. J. Thouless, J. Phys. **C6** (1973), 1181.
- 7) J. M. Kosterlitz, J. Phys. **7** (1974), 1046.
- 8) J. V. José, L. P. Kadanoff, S. Kirkpatrick and D. R. Nelson, Phys. Rev. **B16** (1977), 1217.
- 9) D. M. Lublin, Phys. Rev. Letters **34** (1975), 568.
- 10) A. Luther and D. J. Scalapino, Phys. Rev. **B16** (1977), 1153.
- 11) J. Rogiers and R. Dekeyser, Phys. Rev. **B13** (1976), 4886.
- 12) J. Rogiers and D. D. Betts, Physica **85A** (1976), 553.
D. D. Betts and M. Plischke, Can. J. Phys. **54** (1976), 1553.
- 13) D. D. Betts, Physica **86-88B** (1977), 556.
- 14) R. C. Brower, F. Kuttner, M. Nauenberg and K. Subbarao, Phys. Rev. Letters **38** (1977), 1231.
- 15) R. J. Myerson, Phys. Rev. **B16** (1977), 3203.
- 16) H. Betsuyaku, Solid State Comm. **25** (1978), 185.
- 17) C. Kawabata and K. Binder, Solid State Comm. **22** (1977), 705.
- 18) N. D. Mermin and H. Wagner, Phys. Rev. Letters **17** (1966), 1133.
- 19) M. E. Fisher, J. Vac. Sci and Tech. **10** (1973), 665.
M. E. Fisher and M. N. Barber, Phys. Rev. Letters **28** (1972), 1516.
- 20) M. Suzuki, Prog. Theor. Phys. **58** (1977), 1142.
- 21) S. Ma, Phys. Rev. Letters **37** (1976), 461.
- 22) V. V. Prudnikov and G. B. Teitelbaum, Phys. Letters **63** (1977), 1.